Melting Point Depression of Some Lipids in Pressurized Carbon Dioxide

Ozan N. Ciftci and Feral Temelli*
Department of Agricultural, Food and Nutritional Science
University of Alberta, Edmonton, AB, T6G 2P5 Canada
E-mail: feral.temelli@ualberta.ca, Fax: +1 780 492 8914

ABSTRACT

Understanding the melting behaviour of solid lipids in pressurized carbon dioxide (CO_2) is important for the processing of solid lipids using supercritical CO_2. Melting point depression and volumetric expansion of some solid lipids in pressurized CO_2 was studied as a function of pressure. The highest melting point depression (76.5%) was observed for coconut oil at 43 bar, whereas the lowest was for fully hydrogenated canola oil (FHCO) (18.5%) at 122 bar. The lipids composed of shorter chain fatty acids exhibited higher melting point depression. A positive correlation was observed between the melting point depression and volumetric expansion of the lipids. The lowest expansion was observed for FHCO (9.7%), whereas the highest was for lauric acid (42.7%) at the lowest pressure where the lipids melted.

INTRODUCTION

Major developments have led to new particle formation methods based on supercritical carbon dioxide (SC-CO_2) technologies to deliver pharmaceutical and bioactive substances. Among them, lipid-based particle formation using SC-CO_2 has been receiving growing interest with potential applications in the delivery of drugs and food-related bioactives. Temperature is a key parameter for solid lipid particle production. Processing temperature must be high enough to keep the solid lipid mixture in liquid state during homogenization. However, high temperature melt processing limits the use of heat sensitive bioactives. SC-CO_2–based processes have the potential to overcome such problems by decreasing the melting temperature of the solid lipid.

Generation of melting curves provides useful information demonstrating the pressure and temperature the solid lipid would melt at. Melting point depression in supercritical fluids has been reported for semi-crystalline polymers [1,2] and β-sitosterol [3]. However, the literature on the melting behaviour of solid lipids is scarce. Melting point of cocoa butter (CB) in CO_2 was determined using a modified capillary method in a high pressure optical cell [4] and in a thermostated view cell [5]. Sousa et al. [6] investigated the melting behaviour of lipid matrices in CO_2 using a modified capillary method. Spilimbergo et al. [7] used a high pressure differential scanning calorimeter to study the melting behavior of pure tristearin (TS) in CO_2 and other mixtures only up to 60 bar.

It is evident that the literature lacks information on the melting behavior of solid lipids under SC-CO_2. Therefore, the objective of this study was to investigate the melting behaviour of pure lipids of different classes (TS, trilaurin (TL), monostearin (MS), stearic acid (SA), and lauric acid (LA)) and complex mixtures of real samples (fully hydrogenated canola oil (FHCO), CB, and coconut oil (CO)) in pressurized CO_2 (0-350 bar) in a high pressure view cell using a modified “first melting point” method.

MATERIALS AND METHODS

Materials

Unrefined CO and CB were purchased from a local market. FHCO was kindly provided by Richardson Oilseed Ltd. (Lethbridge, AB). TS (≥80%), TL (≥98%), MS (≥60%), SA (≥95%) and LA (≥98%) were purchased from TCI America (Portland, OR). CO_2 (99.8% bone dry, water level <3 ppm) was obtained from Praxair Canada Inc. (Mississauga, ON).

Determination of Fatty Acid Composition

Fatty acid composition of the CO, CB and FHCO were determined using a gas chromatograph (GC) (Varian 3400, Varian Inc., Walnut Creek, CA) equipped with a flame ionization detector as described previously [8].

Melting Point Measurements in Pressurized CO_2

Melting point measurements were carried out using a phase equilibria apparatus (SITEC-Sieber Engineering AG, Maur/Zurich, Switzerland) described previously [8], but in this case it was equipped with a syringe pump (Model 250D, Teledyne Isco Inc., Lincoln, NE). The temperature of the cell was maintained at 5 °C above the melting point of the lipid sample by circulating water:ethylene glycol mixture (50:50, *V*:*V*) using a refrigerated circulator. Lipids were melted in an oven at 80 °C to erase the crystal memory, and 100 µL of molten fat was loaded into a transparent glass GC vial insert (200 µL, 6 x 28 mm) placed in a transparent 2 mL-GC vial. The GC vial was then placed into the high pressure cell at a position where the sample could be seen by the camera through the sapphire window and then the cap of the cell was closed. After 10 min of equilibration, the cell was gently purged with CO_2 to remove any residual air. Then, the cell was filled with CO_2 and pressurized until the desired level. After equilibration for 1.5 h, the cell was cooled down using the refrigerated circulator until the solidification of the lipid was observed. Phase change of the lipids was visually observed via the real-time image captured by the microscope and the camera. Temperature of the cell was decreased to 5 °C below the observed solidification temperature, and maintained constant at this temperature for 10 min. Then, the temperature of the cell was increased at a heating rate of 1.3 °C min^{-1}. The melting temperature and pressure of the lipid under pressurized CO_2 was recorded as the pressure and temperature at which the first brightness in the picture of the lipid sample during the heating step was observed. It was not possible to observe complete melting of the sample because the bottom of the sample was below the level of the sapphire window.

Measurement of the Volumetric Expansion of Lipids in Pressurized CO_2

Volumetric expansion measurements of the lipid samples in pressurized CO_2 were conducted in the same SITEC phase equilibria unit. In this case, a microscopic glass scale fitted on a stainless steel frame was placed inside the high pressure cell according to Jenab and Temelli [9]. The scale was calibrated using different volumes of water at a sensitivity of 0.05 mm. The temperature of the cell was maintained at the melting temperature at atmospheric pressure of the lipid sample to record initial volume (V_i). Then, the cell was gently flushed with CO_2 and pressurized until the desired level. The mixture was stirred for 2 min and the temperature was decreased to the depressed melting point of the sample at the set pressure based on the previously obtained melting point data (Points A and B). Pressure of the cell decreased during this cooling step and the pressure was adjusted back to the set pressure. After equilibration for 1.5 h with stirring at 600 rpm, the stirrer was turned off and the mixture was allowed to stabilize for 10 min to observe a clear lipid-CO_2 interface, which was recorded as expanded volume (V_e). The volumetric expansion (E, %) was calculated as $[(V_e-V_i)/V_i]*100$.

RESULTS AND DISCUSSION

Melting Point Depression

Figure 1 depicts the melting curve of FHCO in pressurized CO_2, which was typical for all studied lipids. The melting curve was divided into two regions: Region 1 was the linear region where the melting temperature decreased with pressure, while in Region 2 the melting point stayed constant regardless of pressure. Then, melting point depression was determined at a given pressure compared to atmospheric pressure. Figure 2 presents melting point depression of solid lipid standards (TS, TL, MS, SA and LA) with increasing pressure. Higher melting point depression was observed for the lipids containing a shorter chain fatty acid (LA, $C_{12:0}$) compared to those containing a longer chain fatty acid (SA, $C_{18:0}$). Higher-melting point lipids (TS, MS and SA) had a similar trend of melting point depression (Fig. 2), despite the different lipid classes involved, i.e. triacylglycerol, monoacylglycerol and free fatty acid. The transition from Region 1 to Region 2 for the higher-melting point lipids was observed between 100 and 125 bar, and above this pressure range their melting temperature stayed constant. The maximum melting point depression for all the higher-melting point lipids was 18 °C. The pressure needed to reach the maximum melting point depression for lower-melting point lipids (TL and LA) was lower. The transition from Region 1 to Region 2 for TL was observed at 80 bar with a melting point depression of 21 °C, whereas that of LA was 28.2 °C at 67 bar. In terms of percent melting point depression among solid lipid standards, the highest depression was observed for LA (61.3%), followed by TL (45.2%), whereas the lowest was for TS (25.6%), MS (26.3%) and SA (26.8%).

Melting point depression also depended on the lipid classes. The difference between the melting point depression of LA and SA was greater than that of TL and TS (Fig. 2). While there was a big difference between the melting point depression of LA and TL, there was no difference between the melting point depressions of SA, MS and TS. Thus, the fatty acid chain length has the predominant effect on melting point depression, which is due to the different packing properties of fatty acids of varying chain length. The lipids with dense packing have a higher melting point. Long chain fatty acids pack better than short chain ones.

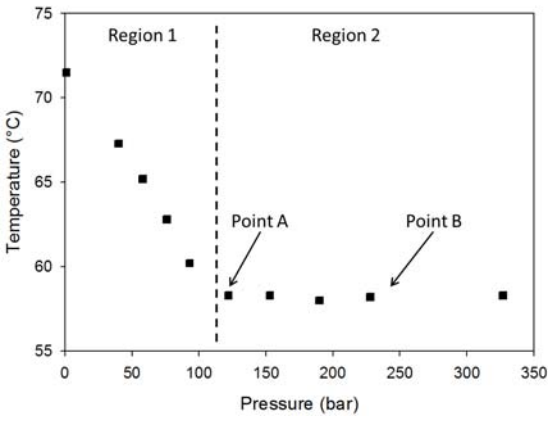

Figure 1: Melting curve of the fully hydrogenated oil in pressurized CO_2, and the points (A and B) at which volumetric expansion was determined

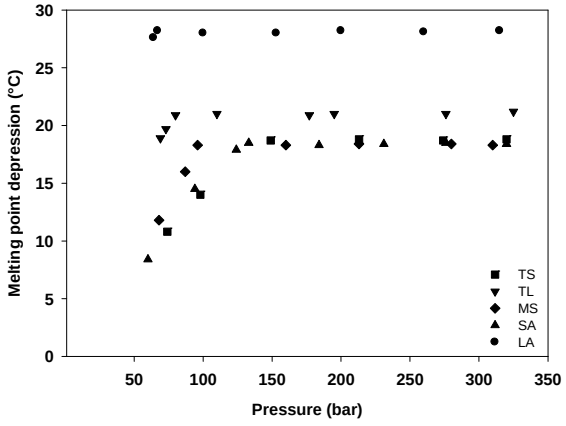

Figure 2. Melting point depression of canola pure lipid standards in pressurized CO_2 as a function of pressure.

Figure 3 presents the melting point depression of the real lipid mixtures FHCO, CO and CB in pressurized CO_2. Similar to the pure lipids, higher melting point depression was observed for the lipids containing a higher fraction of shorter chain fatty acids (Table 1). CO had the highest amount of short chain fatty acids, and thus the highest melting point depression.

Table 1: Fatty acid composition and melting point of the lipids, and the points on the melting curves (Points A and B in Fig. 1) where volumetric expansion of the lipids in pressurized CO_2 was studied.

Lipid	Major fatty acids (%)	Melting point at atmospheric P (°C)	Point A T (°C)/P (bar)	Point B T (°C)/P (bar)
Tristearin		73.0	62.3/149	62.3/243
Monostearin		70.0	51.7/96	52.0/176
Stearic acid		69.0	58.2/133	58.3/224
Trilaurin		46.5	30.0/80	30.0/214
Lauric acid		46.0	26.8/67	28.0/274
Fully hydrogenated canola oil	$C_{16:0}$ 5.0 $C_{18:0}$ 88.2 $C_{18:1}$ 3.3	71.5	58.3/122	58.3/211
Cocoa butter	$C_{16:0}$ 29.8 $C_{18:0}$ 33.3 $C_{18:1}$ 31.8	32.0	21.1/60	21.0/198
Coconut oil	$C_{8:0}$ 8.0 $C_{10:0}$ 6.5 $C_{12:0}$ 50.1 $C_{14:0}$ 18.6 $C_{16:0}$ 8.3 $C_{18:0}$ 2.9 $C_{18:1}$ 4.8	34.0	8.0/43	8.0/200

The melting point of CO decreased by 26 °C with an increase in pressure to 42 bar; however, further increases in pressure up to 350 bar did not cause any further decrease in the melting point (Fig. 3). CB reached the lowest melting point of 21.1 °C at 58 bar with an 11 °C decrease in the melting point. With a higher concentration of longer chain saturated fatty acids (Table 1), CB had a lower melting point depression than CO (34.4% vs 76.5%, relative to that at atmospheric pressure). The pressure needed to decrease the melting point of FHCO was much higher. The maximum decrease in the melting point of FHCO of 13 °C was observed at 122 bar (Fig. 3). Pressures above 122 bar did not cause any further decrease in the melting point of FHCO. The decrease in the melting point of FHCO was 18.5%. The lower melting point depression of FHCO observed at higher pressures was mainly due to its high content of $C_{18:0}$ (88.2%). The transition from Region 1 to Region 2 (Point A in Fig. 1) depended on the fatty acid composition. Point A for CO was observed at the lowest temperature and pressure (Table 1), followed by CB, LA, TL and MS. Although FHCO, SA and TS had similar temperatures at Point A, TS and SA had higher pressures. This was due to the higher purity of SA and TS, which resulted in denser packing.

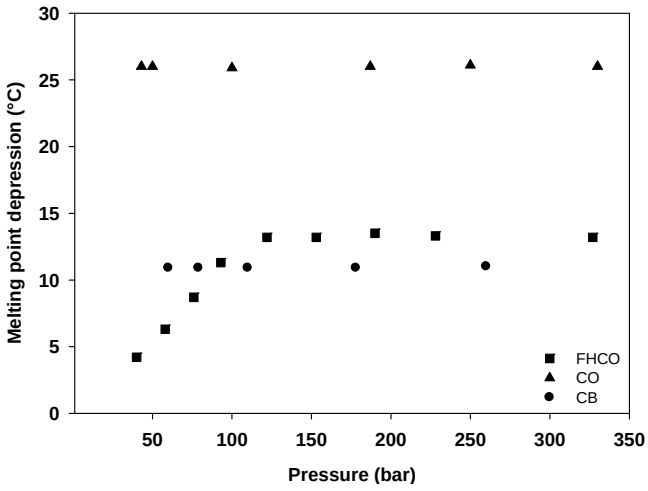

Figure 3: Melting point depression of the complex mixtures of real lipid samples in pressurized CO_2 as a function of pressure.

Volumetric Expansion

Dissolution of CO_2 in the lipids was the main reason for melting point depression, which also resulted in volumetric expansion. The packing of lipids become more disordered due to the dissolution of CO_2 in the liquid lipid. In an attempt to investigate the relationship between the volumetric expansion and the melting point depression, volumetric expansion of the lipids in pressurized CO_2 was studied at two points (Points A and B) along the melting curves as specified in Table 1. In addition, the volumetric expansion was also determined at 63 °C/150 bar for comparison between different samples at fixed conditions.

Figure 4 presents the results for volumetric expansion determined at Points A, B and 63 °C/150 bar. Volumetric expansion of CO at Points A and B could not be measured due to equipment limitations at low temperatures. Volumetric expansion of the lipids increased with pressure at constant temperature. Typically, solubility of CO_2 in the liquid lipid phase increases with pressure up to a certain level and then reaches a plateau [9,10]. Higher volumetric expansions at Point B compared to those at Point A indicated that it is not necessary to have the maximum volumetric expansion to reach the maximum melting point depression. Figure 4 revealed that a certain level of expansion is needed for each lipid to have the maximum melting point depression (Point A), and any further expansion (Point B) after this point does not lead to a change in melting point depression. Region 1 and Region 2 of the melting curves of polymers in pressurized gases are often attributed to "solubility effects" at low pressures, and to "pressure effects" at high pressures [11]. Similarly, the melting point of lipids decreased in Region 1 due to the dissolution of CO_2 with pressure. The presence of CO_2 in the lipid during solidification caused a more disordered packing of the lipid and therefore caused a melting point depression.

The lowest volumetric expansion at Point A was observed for FHCO (9.7%), whereas the highest was for LA (42.7%) (Fig. 4). It was not possible to measure the expansion of the LA at Point B, because it formed a homogeneous mixture with CO_2. LA and SA had higher volumetric expansion compared to their triacylglycerol forms TL and TS, respectively. The highest expansion at 63 °C/150 bar was observed for LA, followed by TL, CO and CB. The lowest expansion was observed for FHCO, TS and SA.

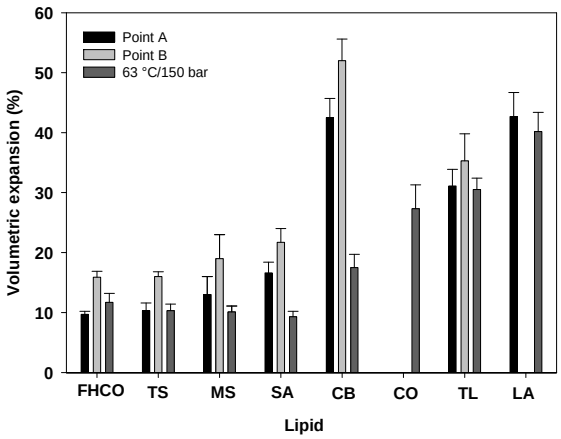

Figure 4: Volumetric expansion of the lipids at Point A, Point B, and 63 °C/122 bar.

CONCLUSIONS

The findings revealed that the melting point of the lipids decreased in pressurized CO_2. Higher melting point depression was observed for the lipids with shorter chain fatty acids. Melting point of the free fatty acids decreased more than their triacylglycerol forms. Similarly, higher volumetric expansion was observed for free fatty acids compared to their triacylglycerol forms. It was shown that the volumetric expansion of the lipids in pressurized CO_2 can be used to obtain information about their melting behaviour in pressurized CO_2.

REFERENCES

[1] LIAN, Z., EPSTEIN, S.A., BLENK, C.W., SHINE, A.D., Journal of Supercritical Fluids, Vol. 39, **2006**, p. 107.
[2] TAKAHASHI, S., HASSLER, J.C., KIRAN, E., Journal of Supercritical Fluids, Vol. 72, **2012**, p. 278.
[3] DOHRN, R., BERTAKIS, E., BEHREND, O., VOUTSAS, E., TASSIOS, D., Journal of Molecular Liquids, Vol. 131–132, **2007**, p. 53.
[4] KOKOT, K., KNEZ, Z., BAUMAN, D., Acta Alimentaria, Vol. 28, **1999**, p. 197.
[5] VENTER, M.J., WILLEMS, P., KARETH, S., WEIDNER, E., KUIPERS, N.J.M., DE HAAN, A.B., Journal of Supercritical Fluids, Vol. 41, **2007**, p. 195.
[6] SOUSA, A.R.S., CALDERONE, M., RODIER, E., FAGES, J., DUARTE, C.M.M., Journal of Supercritical Fluids, Vol. 39, **2006**, p. 13.
[7] SPILIMBERGO, S., LUCA, G., ELVASSORE, N., BERTUCCO, A., Journal of Supercritical Fluids, Vol. 38, **2006**, p. 289.
[8] CIFTCI, O.N., TEMELLI, F., Journal of Supercritical Fluids, Vol. 58, **2011**, p. 79.
[9] JENAB, E., TEMELLI, F., Journal of Supercritical Fluids, Vol. 70, **2012**, p. 57.
[10] SEIFRIED, B., TEMELLI, F., Journal of Supercritical Fluids, Vol. 50, **2009**, p. 97.
[11] KOKOT, K.F., KONIG, A., KNEZ, Z., SKERGET, M., Fluid Phase Equilibria, Vol. 173, **2000**, p. 297.